Large Bulk Photovoltaic Effect and Spontaneous Polarization of Single-Layer Monochalcogenides

Tonatiuh Rangel,[1,2] Benjamin M. Fregoso,[2,3] Bernardo S. Mendoza,[4] Takahiro Morimoto,[2] Joel E. Moore,[2] and Jeffrey B. Neaton[1,2,5]

[1]*Molecular Foundry, Lawrence Berkeley National Laboratory, Berkeley, California 94720, USA*
[2]*Department of Physics, University of California, Berkeley, California 94720, USA*
[3]*Department of Physics, Kent State University, Kent, Ohio 44242, USA*
[4]*Centro de Investigaciones en Óptica, León, Guanajuato 37150, México*
[5]*Kavli Energy Nanosciences Institute at Berkeley, Berkeley, California 94720, USA*

(Received 21 October 2016; published 8 August 2017)

We use a first-principles density functional theory approach to calculate the shift current and linear absorption of uniformly illuminated single-layer Ge and Sn monochalcogenides. We predict strong absorption in the visible spectrum and a large effective three-dimensional shift current ($\sim$100 μA/V^2), larger than has been previously observed in other polar systems. Moreover, we show that the integral of the shift-current tensor is correlated to the large spontaneous effective three-dimensional electric polarization ($\sim$1.9 C/m^2). Our calculations indicate that the shift current will be largest in the visible spectrum, suggesting that these monochalcogenides may be promising for polar optoelectronic devices. A Rice-Mele tight-binding model is used to rationalize the shift-current response for these systems, and its dependence on polarization, in general terms with implications for other polar materials

DOI: 10.1103/PhysRevLett.119.067402

Introduction.—The shift current is a dc current generated in a material under uniform illumination [1–4], and gives rise to phenomena such as the bulk photovoltaic effect (BPVE) [1]. A necessary condition for the BPVE in a material is the lack of inversion symmetry. Interestingly, in the BPVE, the resulting photovoltage is not limited by the band gap energy, and a junction or interface is not required to generate a current. These properties of the BPVE motivate great interest in the possible optoelectronic applications of noncentrosymmetric systems, and they have been suggested to play a role in emerging functional materials, including hybrid halide perovskites [5].

The BPVE is much less studied in two-dimensional (2D) materials [6–8]. Two-dimensional materials represent the ultimate scaling in thickness with mechanical, optical, and electronic properties that are unique relative to their bulk counterparts. For example, single-layer group-IV monochalcogenides GeS, GeSe, SnS, and SnSe are actively being investigated [9–17] due to their band gaps and large carrier mobilities suitable for optoelectronics. Centrosymmetric in the bulk, the monochalcogenides lack inversion symmetry in single-layer form, allowing for the emergence of a spontaneous polarization and a BPVE. Although broken inversion symmetry is necessary for a nonzero shift current, the relationship between shift current and polarization at a given frequency is complex and depends on the degree of asymmetry and spatial localization of the valence and conduction states [5]. On the other hand, the shift-current spectrum integrated over frequency is clearly correlated to polarization, as shown in this Letter.

In this Letter we use first principles density functional theory methods, supplemented by a tight-binding model, to predict and understand the spontaneous polarization and BPVE in single-layered monochalcogenides. In addition to confirming their established favorable band gaps and strong absorption [18,19], we demonstrate that the monochalcogenides exhibit a large in-plane shift current, up to 100 μA/V^2. Using a Rice-Mele tight-binding model, we find that the integral of the frequency-dependent shift-current tensor is

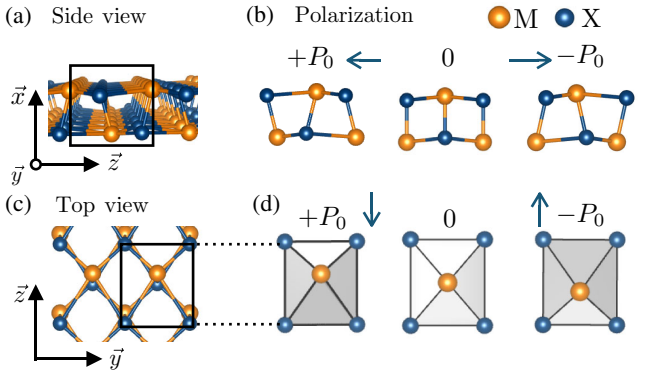

FIG. 1. The crystal structure of single-layer group-IV monochalcogenides MX, where M = Ge, Sn, and X = S, Se. In (a) we show the 3D view of the single-layer and in (b)–(d) the projections of the single-layer crystal on the Cartesian axes. Structures with 0, $\pm P_0$ polarizations are also shown in inset (b) and (d). A twofold rotation along z (plus translations) determines the polarization axis, see text.

TABLE I. Left: Ground state polarization of single-layer monochalcogenides. The 3D effective polarizations are for a layer thickness of $a = 2.6$ Å. The energy barrier between the ground-states with opposite polarization calculated within DFT-PBE are also shown. Right: Direct (D) and indirect (I) band gaps calculated with DFT-PBE and optical gaps reported from *GW*-BSE calculations.

	Polarization		Energy	Supercell			Band gap (eV)			
	2D	3D	barrier	lattice vectors (Å)			DFT-PBE		*GW*-BSE	Expt.[a]
	(nC/m)	(C/m^2)	(K)	a	b	c	D	I	D	D
GeS	0.48	1.9	5563	15.0	3.7	4.5	1.9	1.7	2.2 [19]	1.6 [12]
GeSe	0.34	1.3	1180	15.0	4.0	4.3	1.2	1.2	1.6, 1.3 [18,19]	1.2 [12]
SnS	0.24	0.8	384	15.0	4.1	4.3	1.5	1.4		
SnSe	0.17	0.6	80	15.0	4.3	4.4	0.9	0.9	1.4 [18]	

[a]Experimental optical gaps (Expt.) of few-layer chalcogenides are also shown for comparison

well correlated to the spontaneous polarization; and this integral is maximized at an optimal value of polarization.

Structure, symmetries, and ab initio methods.—Our DFT calculations are performed with the generalized gradient approximation including spin-orbit coupling. We use the ABINIT code [20], with Gaussian pseudopotentials [21] and the Perdew-Burke-Ernzerhof (PBE) functional [22]. We fully relax atomic positions in supercells that include at least 10 Å of vacuum between layers. Our relaxed lattice parameters are shown in Table I and agree with previous work [10] (see details in Supplemental Material [23], which includes Ref. [24]).

Bulk monochalcogenide crystals MX (M = Ge, Sn and X = S, Se) are orthorhombic with point group mmm and space group $Pnma$ (No. 62). They consist of van der Waals-bonded double layers of metal monochalchogenide atoms in an armchair arrangement. The space group of the bulk crystal contains eight symmetries including a center of inversion which prevents spontaneous electric polarization and the BPVE. Upon exfoliation, the resulting single "double layer" primitive cell has four atoms, see Fig. 1. In this work, the layers are chosen to be oriented perpendicular to the x axis as shown in Fig. 1(a). The single-layer structure has four symmetries, including a twofold rotation with respect to z (plus translation), $2[001] + (1/2, 0, 1/2)$, which determines the direction of the in-plane spontaneous polarization of the layer along the z axis. In addition, the 2D system has two mirror symmetries with respect to x and y, $m[100] + (1/2, 1/2, 1/2)$ and $m[010] + (0, 1/2, 0)$. Hence its point group, which determines the nonzero components of the optical response tensors, is $mm2$.

As a consequence of the mirror symmetries with respect to the x and y axis of a single monochalcogenide layer, all the cross-components terms of the imaginary part of the dielectric function, ϵ_2^{ab}, vanish together with the tensor components xxx, xyy, xzz, yxx, yyy, and yzz of the shift current. Only seven components are symmetry allowed [25]: zxx, zyy, zzz, yyz, and xzx, as well as components obtained by interchanging the last two indices. Symmetry, however, does not dictate the magnitude of the response in each direction, and consequently we compute the matrix elements below.

Spontaneous polarization.—We calculate the spontaneous polarization of single-layer chalcogenides using the modern theory of polarization [26,27], as implemented in ABINIT. We first identify an adiabatic path between the ground state and a centrosymmetric geometry with, in this case, zero polarization. We parametrize the atomic displacements along a path between these geometries [Figs. 1(b) and 1(d)] with λ as $\mathbf{R}^i(\lambda) = \mathbf{R}_0^i + \lambda(\mathbf{R}_f^i - \mathbf{R}_0^i)$, where $\mathbf{R}_0^i$ ($\mathbf{R}_f^i$) is the initial (final) position of ith atom in the centrosymmetric (noncentrosymmetric) structure. We calculate the minimum-energy path between the $\pm P_0$ configurations, as detailed in the Supplemental Material [23]. The minimal energy path is indistinguishable from the linear path used here. The polarization for various 2D monochalcogenides has also been theoretically studied recently [13,17,28–33]. Our adiabatic polarization path, is shown schematically in Figs. 1(b) and 1(d). Table I shows the computed spontaneous electric polarization per unit area, $P_0 a$, and an effective 3D polarization assuming an active single-layer thickness $a = 2.6$ Å. Interestingly, GeSe has a significantly higher effective 3D polarization, 1.9 C/m^2, than most prototypical ferroelectrics, e.g., 0.0028 C/m^2 in $CaMn_7O_{12}$ [34], 0.26 C/m^2 in $BaTiO_3$ [35,36], 0.37 C/m^2 in $KNbO_3$ [37], and 0.9 C/m^2 in $BiFeO_3$ [38,39]. The energy barriers, provided in Table I, are much larger than room temperature. However, since reorientation under an applied electric field is often facilitated by domain wall motion, future experiments are necessary to conclusively demonstrate ferroelectric switching behavior.

Optical absorption and shift current.—One notable feature of single-layer monochalcogenides is their promising band gap energies in the visible range [12,18,19]. In Table I, we show the computed DFT-PBE gaps, which are a good estimate of the corresponding optical gaps. Although in principle *ab initio* many-body perturbation theory (MBPT) would be a more rigourous approach to optical gaps, in this case, we expect the PBE single-particle gaps to be indicative since excitonic effects, as large as 1 eV in GeS [19], can fortuitously cancel the well-known tendency of the PBE functional to underestimate the transport gap. In Sn-based materials, the PBE gaps are smaller by ~0.5 eV

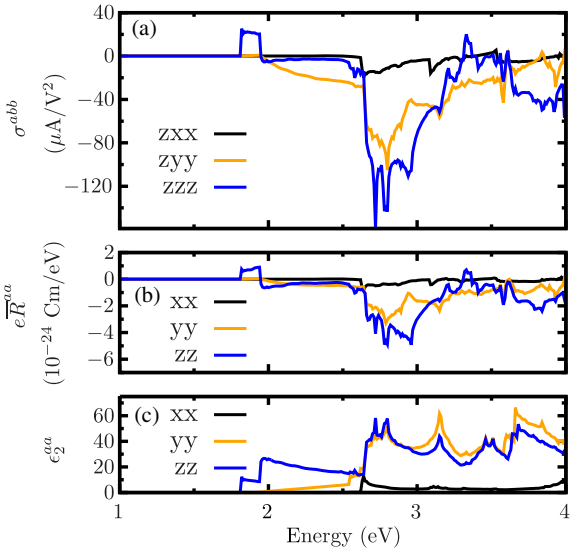

FIG. 2. Shift-current spectra (a), shift vector integrated over $\mathbf{k}$ (b), and linear absorption (c) of single-layer GeS. The large in-plane shift-current response in the visible range is dominated by the shift vector and corresponds to the large absorption along zz and yy.

than in prior MBPT calculations (see Table I), and hence the responses are redshifted and should be treated with more caution. In addition, since exciton formation can alter and even enhance shift current at exciton resonances [40], strong excitonic effects in monochalcogenides could lead to even larger shift currents.

We calculate the imaginary part of the dielectric function, ϵ_2^{ab}, within the independent particle approximation. As shown in Fig. 2, the absorption is strong $\epsilon_2 \sim 50$, in the visible range of 1.5 to 3 eV, due to the direct or nearly direct band gap of these materials [7]. For comparison, we calculate the absorption coefficient $\alpha = \omega\epsilon_2/c$, with light frequency ω and speed of light c. For the 2D monochalcogenides of thickness ~2.6 Å, $\alpha \sim 0.5$–1.5×10^6 cm^{-1}, and similar values were found for graphene and MoS_2 (0.7 and 1–1.5×10^6 cm^{-1}, respectively) [41]. The zz and yy tensor components are larger than xx due to the intrinsic crystal anisotropy, in agreement with previous work [12,18,19]. In addition to the energy gaps and the large absorption in the visible range, single-layer monochalcogenides have a large shift-current response, as shown below.

The dc shift current is generated to second order in the electric field. Consider a monochromatic electric field of the form $E^b(t) = E^b(\omega)e^{i\omega t} + E^b(-\omega)e^{-i\omega t}$. The shift-current response can be expressed in terms of the third-rank tensor $\sigma^{abc}(0;\omega,-\omega)$ as,

$$J^a_{\text{shift}}(\omega) = 2\sum_{bc}\sigma^{abc}(0;\omega,-\omega)E^b(\omega)E^c(-\omega). \quad (1)$$

The shift-current tensor is given by [3]

$$\sigma^{abc}(0;\omega,-\omega) = -\frac{i\pi e^3}{2\hbar^2}\int\frac{d\mathbf{k}}{8\pi^3}\sum_{nm} f_{nm}(r^b_{mn}r^c_{nm;a} + r^c_{mn}r^b_{nm;a})\delta(\omega_{mn}-\omega), \quad (2)$$

where r^a_{mn} are velocity matrix elements. The $r^a_{mn;b}$ are generalized derivatives, defined as $r^a_{mn;b} = \partial r^a_{mn}/\partial k^b - i(A^b_{nn} - A^b_{mm})r^a_{nm}$, where A^a_{nm} are the Berry connections, with the a and b indices denoting Cartesian directions. We define the Fermi-Dirac occupation numbers $f_{nm} = f_n - f_m$, and the band energy differences as $\hbar\omega_{nm} = \hbar\omega_n - \hbar\omega_m$. For linearly polarized incident light, $b = c$, and the integrand in Eq. (2) is proportional to the shift "vector" R^{ab}_{nm} [3], defined as $(1/2)\text{Im}[r^b_{nm}r^b_{mn;a} - r^b_{mn}r^b_{mn;a}]|r^b_{nm}|^{-2}$.

Figure 2 shows the calculated effective shift-current spectra for GeS parallel and perpendicular to the polarization axis. (The shift-current spectra for GeSe, SnS, and SnSe have similar features, see the Supplemental Material [23].) We report the responses assuming an active single-layer thickness of $a = 2.6$ Å [42]. We find a broad maximum of the order of 100 μA/V^2 which, importantly, occurs in the visible range (1.5–3.3 eV). The in-plane components, zzz and zyy, are larger than the out-of-plane component zxx, consistent with the large absorption along zz and yy. We compare this response with that of prototypical ferroelectric materials in the same frequency range, e.g., 0.05 μA/V^2 in $BiFeO_3$ [5], and 5 μA/V^2 in $BaTiO_3$ [5], which are much smaller. Additionally, 0.5 μA/V^2 is reported for hybrid halide perovskites [5] and $NaAsSe_2$ [44], and 250 μA/V^2 (= 400 mA/W) is found for state-of-the-art Si-based solar cells [45] (see the Supplemental Material [23] for details on the conversion between shift-current and A/W units). The BPVE for 2D monochalcogenides is therefore quite large.

The absorption and shift-current spectra are related by the velocity matrix elements r_{nm} entering Eq. (2), explaining why peaks in ϵ_2 tend to correspond to peaks in the shift current spectra. To explore the relationship between ϵ_2^{bb} and σ^{abb}, in Fig. 2(b), we plot the shift vector integrated over the Brillouin zone (BZ) [5,46],

$$e\bar{R}^{ab}(\omega) = e\Omega\int\frac{d\mathbf{k}}{8\pi^3}\sum_{nm} f_{nm}R^{ab}_{nm}\delta(\omega_{nm}-\omega), \quad (3)$$

where Ω is the volume of the unit cell.

For the monochalcogenides, $e\bar{R}^{bb}(\omega)$ contains most features of $\sigma^{abb}(\omega)$, and hence dominates the shift-current response. Following the analysis of Ref. [46], we interpret $e\bar{R}^{ab}$ as a collective shift of polarization upon excitation, due to transitions from valence to conduction states with a distinct center of mass [47]. Thus, wave function Berry phases play a fundamental role in the BPVE, which we further explore next.

Polarization and shift current.—To understand the relation between σ^{abb} and polarization P, consider a short-circuit

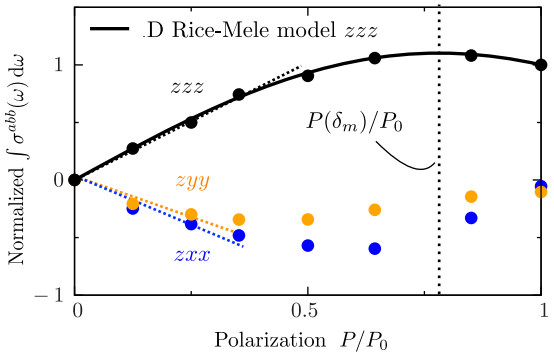

FIG. 3. Nonmonotonic dependence of the integral of the shift-current tensor vs electric polarization for GeS; the integral is normalized by -3×10^{10} $\mathrm{As^{-1}\,V^{-2}}$, its value at the ground state with polarization $P_0 = 1.9$ $\mathrm{C/m^2}$. The tensor components zzz, zyy, and zxx are shown in black, green, and blue points, respectively. For small P the integral is directly proportional to polarization (dashed lines), but it is nonmonotonic for large P. The integral reaches it maxima at $P(\delta_m)$, which is close to P_0.

bulk ferroelectric illuminated by unpolarized light with a flat broad spectrum. The short-circuit current in the z direction, $I_{\mathrm{sc}} = AE_0^2\int d\omega[\sigma^{zyy}(0;\omega,-\omega)+\sigma^{zzz}(0;\omega,-\omega)]$, is proportional to the integral of the shift current tensor. Here, the cross sectional area is A and the amplitude of the electric field is E_0. To first nonvanishing order in λ, both the polarization and the integral are linear in λ, $P(\lambda)=\partial_\lambda P(0)\lambda+\cdots$, $\int\sigma^{abb}(\lambda)=(\int\partial_\lambda\sigma^{abb}(0))\lambda+\cdots$, and hence proportional to each other.

In Fig. 3 we show the integral of the shift-current tensor over the frequency range (up to 6 eV) for GeS as a function of polarization along the adiabatic path of Fig. 1(b). For small polarization, the integral grows linearly with polarization, as expected. However, for larger polarization there is nonmonotonic behavior which we explain below with a tight-binding model. Notice that without the integral, the expansion coefficients become frequency dependent and the current could increase or decrease with polarization with no general relationship.

The Rice-Mele tight-binding model.—As mentioned previously, the monochalcogenide layer has a $2[001]+(1/2,0,1/2)$ symmetry that transforms the upper three atoms in Fig. 1(b) onto the lower three. This suggests there is an effective one-dimensional description of the armchair structure in the z direction, and in fact, as we show below, the trends in the integral of the shift-current tensor along z are captured by a simple model Rice-Mele (RM) model [48,49]. The RM Hamiltonian is

$$H=\sum_i\left[\left(\frac{t}{2}+(-1)^i\frac{\delta}{2}\right)(c_i^\dagger c_{i+1}+\mathrm{H.c.})+(-1)^i\Delta c_i^\dagger c_i\right], \tag{4}$$

where δ parametrizes the structural distortion relative to the centrosymmetric structure, Δ the staggered on-site potential, and $c_i^\dagger$ is the creation operator for electrons at site i. Inversion symmetry is broken when both $\Delta\neq0$ and $\delta\neq0$, and preserved otherwise. For this two-band model Eq. (2) gives (see the Supplemental Material [23] for more details)

$$\int d\omega\sigma^{zzz}(0;\omega,-\omega)=e^3\int dk\frac{|v_{cv}|^2R_{cv}}{4E^2}, \tag{5}$$

where $R_{cv}=\partial\phi_{cv}/\partial k+A_{cc}-A_{vv}$ is the shift vector and is gauge invariant. $A_{nm}=i\langle u_n|\partial_k|u_m\rangle$ are the Berry connections, and ϕ^b_{nm} is defined by $r^b_{nm}=|r^b_{nm}|e^{-i\phi^b_{nm}}$, where $E(k)$ is the band dispersion and v_{cv} is the matrix element of the velocity operator. The Rice-Mele model allows for a complete analytic solution for the optical response and these results will be presented elsewhere [50]. The polarization is $P(\delta)=(e/2\pi)\int dk[A_{vv}(k,\delta)-A_{vv}(k,0)]$. The model has two independent parameters δ and Δ. To make contact with the monochalcogenides, we set $t=1$, and δ and Δ are related by the energy gap, $2\sqrt{\delta_0^2+\Delta_0^2}=1.9$ eV (for GeS). Choosing parameters $(t,[0,\delta_0],\Delta_0)=(1,[0,-0.87],0.4)$ eV fits the zzz *ab initio* integral for GeS well and corresponds to a gap of 1.9 eV. The RM model polarization is $P_0=P(\delta_0)$.

As the RM model is a good description of the integral of the shift-current tensor in monochalcogenides, we now explore the relation between polarization and shift current within this model. The integral of the shift current tensor in Eq. (5) is determined by the competition between the shift vector and the velocity matrix elements $\hbar^2|v_{cv}|^2/4E^2\equiv|r_{cv}|^2$. These in turn are controlled by δ and Δ, which have opposing tendencies: whereas increasing Δ tends to localize charge at lattice sites, increasing dimerization δ moves the center of charge away from them (leading to an increase in polarization). We find that for $\delta\ll\Delta$, R_{cv} is sharply peaked at $k=0$ but $|v_{cv}|^2/4E^2$ peaks at π/c, and hence the integral is small. As δ increases, R_{cv} and $|v_{cv}|^2/4E^2$ broaden, and the integral increases; the integral reaches a maximum at an optimum value, $\pm\delta_m$ which to lowest order in Δ is

$$\delta_m=\Delta+O(\Delta^3\log\Delta), \tag{6}$$

where the polarization takes the value $P(\delta_m)$. For GeS, GeSe, and SnS, δ_0 (-0.9, -0.5, and -0.6 respectively) is relatively close to the optimal δ_m values of -0.5, -0.5, and -0.6, respectively, whereas for SnSe, δ_m (0.4) is farthest from δ_0 (-0.2), see the Supplemental Material [23]. Therefore, consistent with Refs. [7] and [5], the large shift current in these monochalcogenides results from two competing factors, a large shift vector and large velocity matrix elements (linear absorption strength), both of which can be modulated with polarization (and therefore composition, structure, and external electric field).

Discussion and conclusions.—We have calculated the shift-current response and spontaneous electric polarization of a family single-layer monochalcogenides, MX, where M = Ge, Sn, and X = S, Se. We find a large shift current and a large polarization compared with prototypical ferroelectric materials. The fact that the maximum current occurs in the visible range highlights the potential of these materials for optoelectronic applications. Further, the large spontaneous polarization can serve as a knob to engineer the photoresponse. The integral of the shift-current tensor over frequency is clearly dependent on polarization and by means of a RM model, we find an optimal value of polarization where the current is maximum.

We thank J. Sipe, F. de Juan, S. Barraza-Lopez, S. Coh, R. A. Muniz, and S. E. Reyes-Lillo for useful discussions. This work is supported by the U.S. Department of Energy, Director, Office of Science, Office of Basic Energy Sciences, Materials Sciences and Engineering Division, under Contract No. DE-AC02-05CH11231, through the Theory FWP (KC2301) at Lawrence Berkeley National Laboratory (LBNL). B. M. F. acknowledges support from AFOSR MURI, Conacyt, and NERSC Contract No. DE-AC02-05CH11231. This work is also supported by the Molecular Foundry through the DOE, Office of Basic Energy Sciences under the same contract number. T. M. acknowledges support from the Gordon and Betty Moore Foundation's EPiQS Initiative Theory Center Grant. J. E. M. acknowledges Laboratory Directed Research and Development (LDRD) funding from LBNL Contract No. DEAC02-05CH11231. B. S. M. acknowledges partial support from CONACYT-Mexico GoGa No. 153930. We acknowledge the use of computational resources at the NERSC.

B. M. F. and T. R. contributed equally to this work.

[1] B. I. Sturman and P. J. Sturman, *Photovoltaic and Photorefractive Effects in Noncentrosymmetric Materials* (CRC Press, Boca Raton, Florida, 1992).
[2] R. von Baltz and W. Kraut, Phys. Rev. B **23**, 5590 (1981).
[3] J. E. Sipe and A. I. Shkrebtii, Phys. Rev. B **61**, 5337 (2000).
[4] L. Z. Tan, F. Zheng, S. M. Young, F. Wang, S. Liu, and A. M. Rappe, npj Comput. Mater. **2**, 16026 (2016).
[5] S. M. Young, F. Zheng, and A. M. Rappe, Phys. Rev. Lett. **109**, 236601 (2012); S. M. Young and A. M. Rappe, Phys. Rev. Lett. **109**, 116601 (2012); F. Zheng, H. Takenaka, F. Wang, N. Z. Koocher, and A. M. Rappe, J. Phys. Chem. Lett. **6**, 31 (2015); S. M. Young, F. Zheng, and A. M. Rappe, Phys. Rev. Applied **4**, 054004 (2015).
[6] A. Zenkevich, Y. Matveyev, K. Maksimova, R. Gaynutdinov, A. Tolstikhina, and V. Fridkin, Phys. Rev. B **90**, 161409 (2014).
[7] A. M. Cook, B. M. Fregoso, F. de Juan, and J. E. Moore, Nat. Commun.**8**, 14176 (2017).
[8] Y. B. Lyanda-Geller, S. Li, and A. V. Andreev, Phys. Rev. B **92**, 241406 (2015).
[9] L. Li, Z. Chen, Y. Hu, X. Wang, T. Zhang, W. Chen, and Q. Wang, J. Am. Chem. Soc. **135**, 1213 (2013).
[10] A. K. Singh and R. G. Hennig, Appl. Phys. Lett. **105**, 042103 (2014).
[11] F. Wang, S. M. Young, F. Zheng, I. Grinberg, and A. M. Rappe, Nat. Commun. **7**, 10419 (2016).
[12] P. Ramasamy, D. Kwak, D.-H. Lim, H.-S. Ra, and J.-S. Lee, J. Mater. Chem. C **4**, 479 (2016).
[13] M. Wu and X. C. Zeng, Nano Lett. **16**, 3236 (2016).
[14] C. Kamal, A. Chakrabarti, and M. Ezawa, Phys. Rev. B **93**, 125428 (2016).
[15] S.-D. Guo, and Y.-H. Wang, J. Appl. Phys. **121**, 034302 (2017).
[16] C. Xin, J. Zheng, Y. Su, S. Li, B. Zhang, Y. Feng, and F. Pan, J. Phys. Chem. C **120**, 22663 (2016).
[17] P. Z. Hanakata, A. Carvalho, D. K. Campbell, and H. S. Park, Phys. Rev. B **94**, 035304 (2016).
[18] G. Shi and E. Kioupakis, Nano Lett. **15**, 6926 (2015).
[19] L. C. Gomes, P. E. Trevisanutto, A. Carvalho, A. S. Rodin, and A. H. C. Neto, Phys. Rev. B **94**, 155428 (2016).
[20] X. Gonze *et al.*, Comput. Phys. Commun. **205**, 106 (2016).
[21] M. Krack, Theor. Chem. Acc. **114**, 145 (2005).
[22] J. P. Perdew, K. Burke, and M. Ernzerhof, Phys. Rev. Lett. **77**, 3865 (1996).
[23] See Supplemental Material at http://link.aps.org/supplemental/10.1103/PhysRevLett.119.067402 for details on numerical calculations of shift current spectra for GeSe, GeS, SnS and SnSe.
[24] F. Nastos, J. Rioux, M. Strimas-Mackey, B. S. Mendoza, and J. E. Sipe, Phys. Rev. B **76**, 205113 (2007).
[25] P. N. Butcher, *Nonlinear Optical Phenomena* (Engineering Experiment Station of the Ohio State University, Columbus, OH, 1965).
[26] D. Vanderbilt and R. D. King-Smith, Phys. Rev. B **48**, 4442 (1993).
[27] R. Resta, J. Phys. Condens. Matter **22**, 123201 (2010).
[28] L. C. Gomes, A. Carvalho, and A. H. C. Neto, Phys. Rev. B **92**, 214103 (2015).
[29] R. Fei, W. Li, J. Li, and L. Yang, Appl. Phys. Lett. **107**, 173104 (2015).
[30] M. Mehboudi, B. M. Fregoso, Y. Yang, W. Zhu, A. van der Zande, J. Ferrer, L. Bellaiche, P. Kumar, and S. Barraza-Lopez, Phys. Rev. Lett. **117**, 246802 (2016).
[31] R. Fei, W. Kang, and L. Yang, Phys. Rev. Lett. **117**, 097601 (2016).
[32] M. Mehboudi, A. M. Dorio, W. Zhu, A. van der Zande, H. O. H. Churchill, A. A. Pacheco-Sanjuan, E. O. Harriss, P. Kumar, and S. Barraza-Lopez, Nano Lett. **16**, 1704 (2016).
[33] H. Wang and X. Qian, 2D Mater. **4**, 015042 (2017).
[34] R. D. Johnson, L. C. Chapon, D. D. Khalyavin, P. Manuel, P. G. Radaelli, and C. Martin, Phys. Rev. Lett. **108**, 067201 (2012).
[35] A. von Hippel, Rev. Mod. Phys. **22**, 221 (1950).
[36] J. Shieh, J. Yeh, Y. Shu, and J. Yen, Mater. Sci. Eng. C **161**, 50 (2009).
[37] R. Resta, M. Posternak, and A. Baldereschi, Phys. Rev. Lett. **70**, 1010 (1993).
[38] J. B. Neaton, C. Ederer, U. V. Waghmare, N. A. Spaldin, and K. M. Rabe, Phys. Rev. B **71**, 014113 (2005).
[39] G. Catalan and J. F. Scott, Adv. Mater. **21**, 2463 (2009).

[40] T. Morimoto and N. Nagaosa, Phys. Rev. B **94**, 035117 (2016).
[41] M. Bernardi, M. Palummo, and J. C. Grossman, Nano Lett. **13**, 3664 (2013).
[42] Here we show that a single-layer monochalcogenide has a large shift current response, moreover, in the Supplemental Material [23] we show that the response of a thick 3D array of slabs, characterized by the Glass coefficient [43], is also large.
[43] A. M. Glass, D. v. d. Linde, and T. J. Negran, Appl. Phys. Lett. **25**, 233 (1974).
[44] J. A. Brehm, S. M. Young, F. Zheng, and A. M. Rappe, J. Chem. Phys. **141**, 204704 (2014).
[45] M. Pagliaro, G. Palmisano, and R. Ciriminna, *Flexible Solar Cells* (Wiley-VCH, Weinheim, 2008).
[46] B. M. Fregoso, T. Morimoto, and E. J. Moore, arXiv: 1701.001.
[47] The integral of the shift vector over $\mathbf{k}$, $\bar{R}$ has been studied for complex ferroelectric materials, such as $BiTiO_3$ and $PbTiO_3$ in Ref. [5].
[48] D. Vanderbilt and R. D. King-Smith, Phys. Rev. B **48**, 4442 (1993).
[49] S. Onoda, S. Murakami, and N. Nagaosa, Phys. Rev. Lett. **93**, 167602 (2004).
[50] B. M. Fregoso *et al.* (to be published).